Title: Refractory for Black Liquor Gasifiers

Type of Report: Topical Report Task 1.2

Reporting Period Start Date: October 1, 2003

Reporting Period End Date: March 30, 2004

Principal Authors: William L. Headrick Jr., Musa Karakus and Alireza Rezaie

Date Report Issued: June 2004

DOE Award Number: DE-FC26-02NT41491

Name and Address of Submitting Organization:
Curators of the University of Missouri on behalf of University of Missouri-Rolla
Sponsored Programs
1870 Miner Circle
215 ME Annex
Rolla, MO 65409-1330

DISCLAIMER

ABSTRACT

The University of Missouri-Rolla will identify materials that will permit the safe, reliable and economical operation of combined cycle gasifiers by the pulp and paper industry. The primary emphasis of this project will be to resolve the material problems encountered during the operation of low-pressure high-temperature (LPHT) and low-pressure low-temperature (LPLT) gasifiers while simultaneously understanding the materials barriers to the successful demonstration of high-pressure high-temperature (HPHT) black liquor gasifiers. This study will define the chemical, thermal and physical conditions in current and proposed gasifier designs and then modify existing materials and develop new materials to successfully meet the formidable material challenges. Resolving the material challenges of black liquor gasification combined cycle technology will provide energy, environmental, and economic benefits that include higher thermal efficiencies, up to three times greater electrical output per unit of fuel, and lower emissions. In the near term, adoption of this technology will allow the pulp and paper industry greater capital effectiveness and flexibility, as gasifiers are added to increase mill capacity. In the long term, combined-cycle gasification will lessen the industry's environmental impact while increasing its potential for energy production, allowing the production of all the mill's heat and power needs along with surplus electricity being returned to the grid. An added benefit will be the potential elimination of the possibility of smelt-water explosions, which constitute an important safety concern wherever conventional Tomlinson recovery boilers are operated.

Developing cost-effective materials with improved performance in gasifier environments may be the best answer to the material challenges presented by black liquor gasification. Refractory materials may be selected/developed that either react with the gasifier environment to form protective surfaces in-situ; are functionally-graded to give the best combination of thermal, mechanical, and physical properties and chemical stability; or are relatively inexpensive, reliable repair materials. Material development will be divided into 2 tasks:

Task 1, Development and property determinations of improved and existing refractory systems for black liquor containment. Refractory systems of interest include magnesium aluminate and barium aluminate for binder materials, both dry and hydratable, and materials with high alumina contents, 85-95 wt%, aluminum oxide, 5.0-15.0 wt%, and BaO, SrO, CaO, ZrO_2 and SiC.

Task 2, Finite element analysis of heat flow and thermal stress/strain in the refractory lining and steel shell of existing and proposed vessel designs. Stress and strain due to thermal and chemical expansion has been observed to be detrimental to the lifespan of existing black liquor gasifiers. The thermal and chemical strain as well as corrosion rates must be accounted for in order to predict the lifetime of the gasifier containment materials.

TABLE OF CONTENTS

LIST OF GRAPHICAL MATERIALS

INTRODUCTION

Worldwide growth of black liquor production as a new source of energy and electricity necessitates the development of new refractory materials resistant to harsh operating conditions of black liquor gasifiers. Black liquor is a by-product of the papermaking process. Black liquor is an aqueous solution containing waste organic material, which is mainly lignin, as well as the spent pulping chemicals, which are primarily sodium carbonate and sodium sulfide [1]. Chemical energy can be recovered from black liquor by burning it as a liquid fuel in a boiler or gasifier [1, 2]. Black Liquor Gasification (BLG) is widely viewed as the technology that will replace the recovery boiler in the pulp and paper industry [3]. Similar gasification processes are used to convert low-cost solids such as biomass or waste liquids into clean-burning gases [3]. Combustion of these gases has the potential to partially or fully meet the energy needs for pulp and paper plants, reducing or eliminating dependence on electricity generated commercially by the combustion of fossil fuels [4]. The fundamentals of the gasification process have been reviewed elsewhere [4]. The scope of this project will be on high temperature process (900-1000ºC) developed by Chemrec [5]. The operating conditions of the process were studied in Task 1.0 and thermodynamic analysis was performed based upon the results of this study.

Thermodynamics based on chemical analysis showed that the composition of black liquor smelt that would contact the refractory lining is 70-75% Na_2CO_3 (T_m=858°C), 20-25% Na_2S (T_m=1172°C) and 2-5% K_2CO_3 (T_m=901°C). To date, aluminosilicate or fused cast alumina-based materials have been used in this application. Both thermodynamic calculations and experience show that these aluminosilicates are not sufficiently resistant to the alkali containing atmospheres for extended operation of gasifiers. Thermodynamic analysis showed that oxides such as magnesia, ceria and zirconia or aluminates such as barium and lithium aluminate may have satisfactory stability against black liquor smelt. Non-oxides such as SiC and Si_3N_4 were dissolved by black liquor smelt and were not candidates for this application. The objective of task 1.2 was to verify the results of thermodynamics by experiments.

EXPERIMENTAL PROCEDURE

Sessile drop testing was employed to measure the contact angle between the candidate refractory materials and black liquor components. The thermodynamics of interaction of the materials with black liquor smelt was studied before [6]. The schematic of the equipment used for sessile drop testing is presented in Figure 1. The system was designed for the precise determination of the contact angle of liquid droplets on solid substrates under controlled conditions of temperature and atmosphere. The main features of the system are the sessile drop furnace, the controlled atmosphere and the image acquisition system. The furnace was a horizontal tube furnace, resistant heated with Ni-chrome wire with a high-purity, dense and impermeable mullite reaction tube. Each candidate material substrate was placed on an alumina D-tube which was positioned at the center at the hot zone. The experiments were carried out in argon atmosphere. Sample temperature was controlled to within ±5°C as measured with a K-type thermocouple. An optical-quality, fused quartz window permitted observation of the in-situ sessile drop and video recording of the interface interaction behavior between the substrate and the smelt.

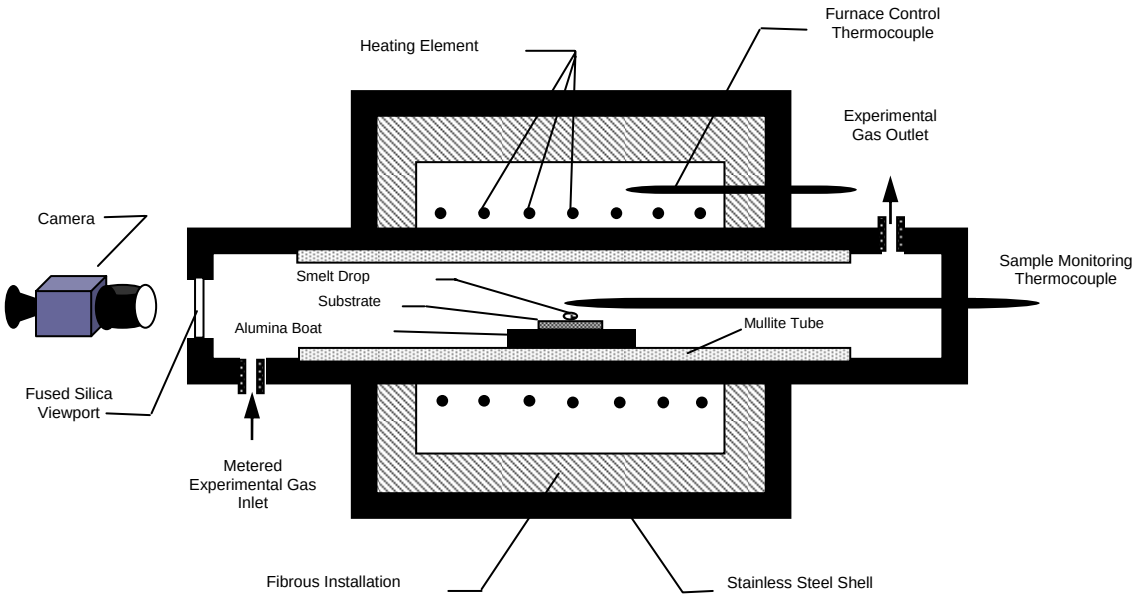

Figure 1: Sessile drop test equipment to measure the contact angle

In sessile drop experiments, smelt powder (0.2-0.3 g), sodium carbonate and potassium carbonate, was formed into 1/4" diameter cylindrical geometry by uniaxial pressing using a 1/4" stainless steel die. The formed smelt powder was placed on the substrate and the liquid drop was formed by heating the drop to 1000°C in 2.5 hours and maintained at 1000°C for 10 hours. Long soaking time was selected to overcome the kinetic barrier and let the sample react with the smelt if there was no thermodynamic barrier. The image of the sessile drop was recorded by a camera and the contact angle was measured at the temperature of complete melting of the drop using enlargement of a photograph extracted from recorded video film of entire test. The average of the 5-7 values was taken as the contact angle.

After cooling from the final sessile drop test temperature (1000°C), the interaction between the solidified smelt and the substrate was examined by thin film x-ray diffraction. If the results of thin film analysis were not satisfactory, the mixture of the powder of each candidate with smelt powder was heated to 1000°C under the same conditions as the sessile drop test. The reaction products were ground to “-200” mesh powder and analyzed by x-ray diffraction. The interface was also examined in a scanning electron microscope (SEM; Hitachi S-570) and with energy dispersive x-ray analysis by sectioning the substrate across the interface but it was not possible to determine the depth of reaction with scanning electron microscopy, as the contrast between the original oxides and the reaction products was not high enough to accurately estimate a reaction depth. In addition, energy dispersive spectrometry could not adequately detect sodium, a relatively light element close to the detection limit of the apparatus. Moreover, because sessile drop test is not an appropriate test to do kinetic studies on corrosion and compare the resistance of different materials, a simulative corrosion test such as finger test will be used to study the resistance of different materials to react with black liquor. If x-ray diffraction analysis doesn’t show any reaction of the material with black liquor or the constituents, kinetic studies of the reaction do not seem meaningful. In this case, only

microstructural features such as porosity, grain size or impurity will affect the corrosion kinetics.

The substrates of Al_2O_3, MgO and CeO_2 candidate materials were formed in 3/4" diameter and 0.2-0.4" height of high purity powder (>99.5%) , sintered at 1600°C for 2 hours to get to about 95% of the theoretical density with almost no open porosity. The substrates of mullite ($3Al_2O_3.2SiO_2$), Y_2O_3, ZrO_2, $MgAl_2O_4$, $LiAlO_2$ were fabricated in cylindrical shape with 1.5" diameter and 0.1-0.2" height to obtain 97% of theoretical density and no open porosity. The surface of each substrate was ground using sand paper and then polished with diamond paste down to 1μm to form a smooth surface required to measure the contact angle. The open porosity and the density (relative to theoretical density) of each substrate measured by Archimedes method is reported in Figure 2 and 3.

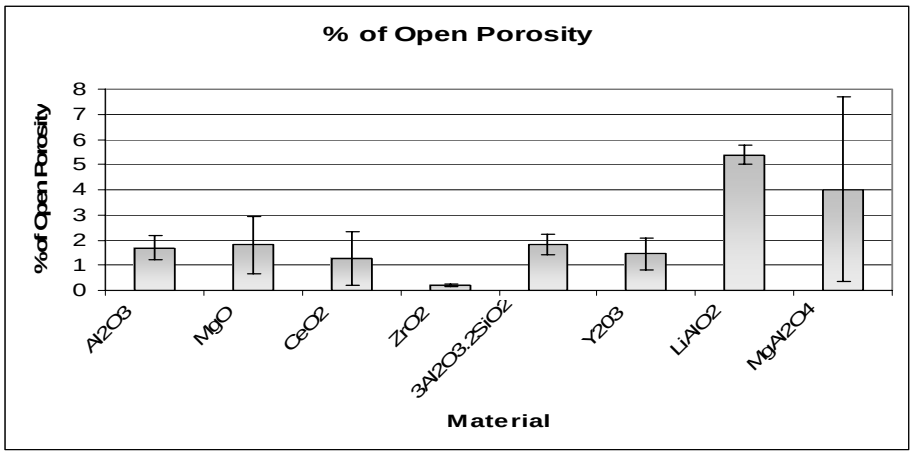

Figure 2: % of open porosity of the substrates used in sessile drop testing

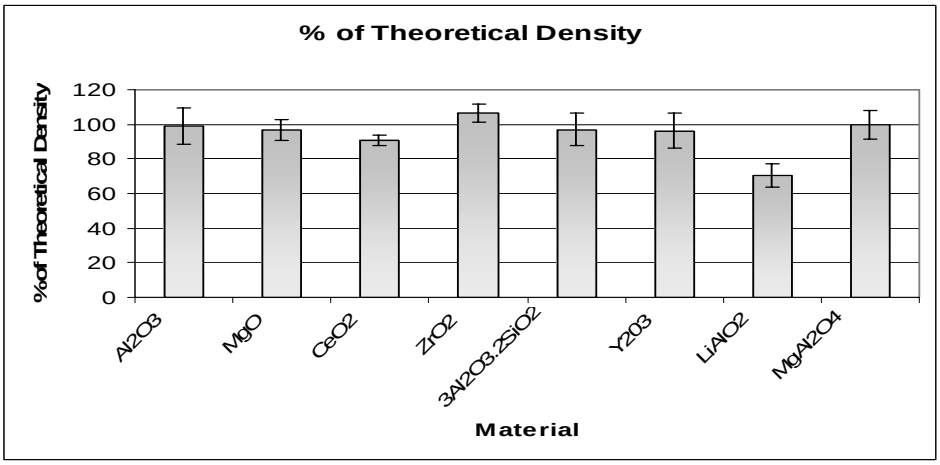

Figure 3: % of theoretical density of the substrates used in sessile drop test

Among different selected materials, only $LiAlO_2$ and CeO_2 didn't have satisfactory density. But when the % of open porosity is also considered and compared with the % of theoretical density, it is concluded that most of the porosity of the specimen is closed porosity which doesn't have considerable effect on the results of sessile drop testing.

RESULTS AND DISCUSSION

Figure 4 shows a schematic of smelt/specimen interface and measurement of the contact angle. The part of the substrate used to be analyzed by x-ray diffraction and studied by SEM is shown as well.

Figure 5 shows the x-ray diffraction pattern of the commercial black liquor supplied by the Weyerhaeuser BLG plant in North Carolina. This pattern verified the results of thermodynamics and showed that black liquor smelt is mainly composed of sodium carbonate and sodium sulfide. Potassium carbonate was not definitely detected due to either insufficient amount in the composition or background noise in the pattern. Sodium oxide in another phase which may exist in black liquor smelt. The other phase that may match the peaks of pattern obtained from the black liquor smelt is sulfur oxide graphite (C_2SO_3) which was not expected by thermodynamics; however, many peaks were unidentified.

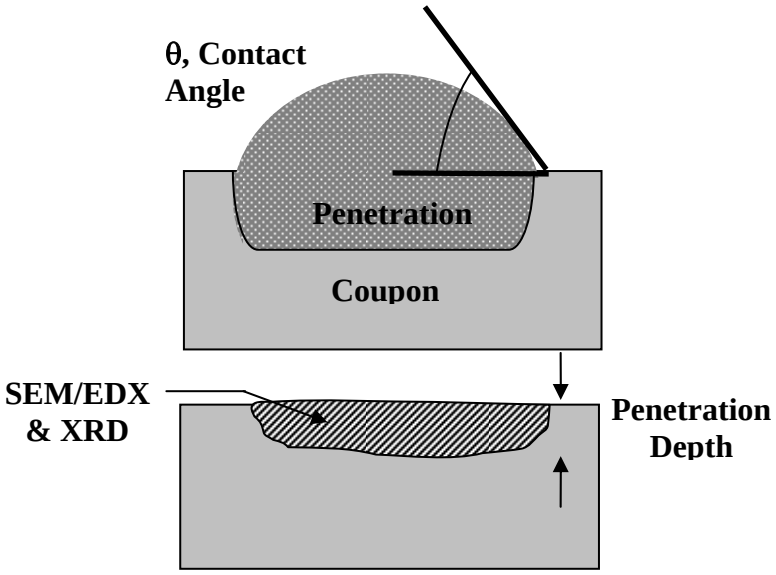

Figure 4: Schematic of contact angle measurement and part of sample analyzed by XRD and SEM/EDX

Sessile drop testing was accomplished with sodium carbonate and potassium carbonate since they are in liquid state at operating temperature of black liquor gasification but sodium sulfide is not.

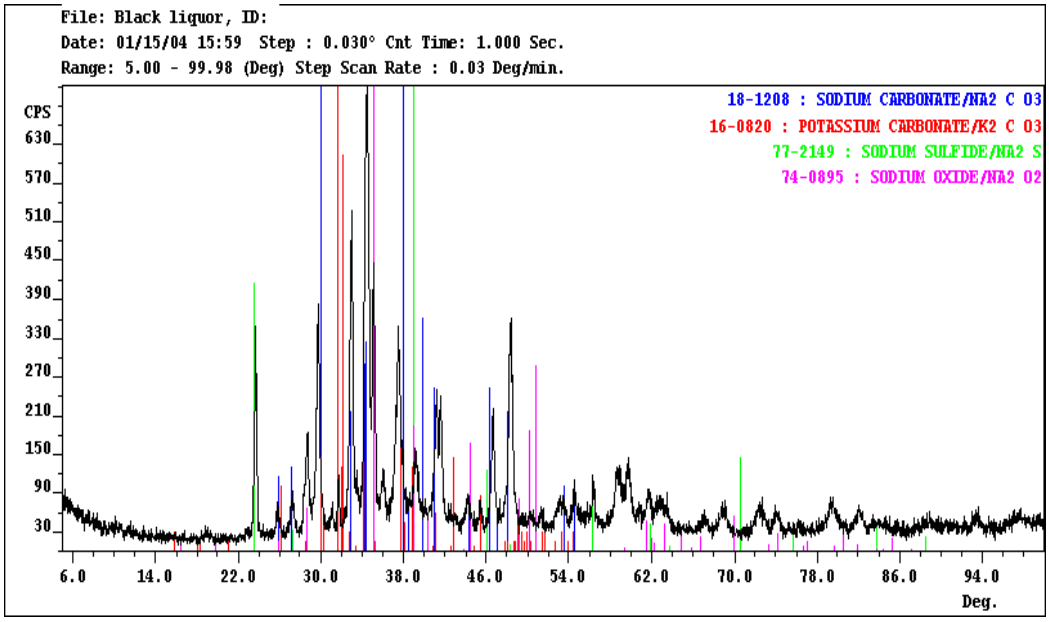

Figure 5: X-ray pattern of black liquor smelt

Figure 6 is a presentation of measured contact angle between the candidate materials and sodium carbonate under argon atmosphere at 1000°C. $MgAl_2O_4$ (spinel) specimen had the highest contact angle (13 ± 1 degrees), but it was still wet by the sodium carbonate. It was expected that the sodium carbonate would wet all oxide refractories. Figure 7 shows Na_2CO_3 drop on spinel substrate at the time it was completely molten and when the measurement was accomplished. Figure 8 shows Na_2CO_3 drop on mullite substrate under the same conditions. The difference of wetting behavior of spinel and mullite with Na_2CO_3 is considerable and distinguishable clearly. Lithium aluminate specimen cracked during sessile drop testing probably due penetration of sodium carbonate through grain boundaries and reaction with the specimen. Results of x-ray diffraction of a powder mixture of lithium aluminate and sodium carbonate at 1000°C under argon atmosphere showed no reaction which is in contradiction with the results of x-ray diffraction obtained from the surface of lithium aluminate disc exposed to sodium carbonate melt in sessile drop testing. Formation of sodium aluminate and specific volume increase of new compound compared to the original phase resulted in the formation of crack in the structure of the material and failure of the specimen. Measurement of contact angle of lithium aluminate with sodium carbonate melt was not possible due to early reaction of the substrate with the melt and crack formation. Formation of crack specifically in grain boundaries is presented in figure 9, 10 and 11. The grain edge areas or the areas close to the grain boundaries with brighter phase shows more sodium in the composition compared to the grain compositions. The qualitative EDS technique verifies the formation of sodium containing phases close to grain boundaries compared to grain composition (Figure 12 and 13). Sodium can either form sodium aluminate or can be dissolved in lithium aluminate and form a solid solution.

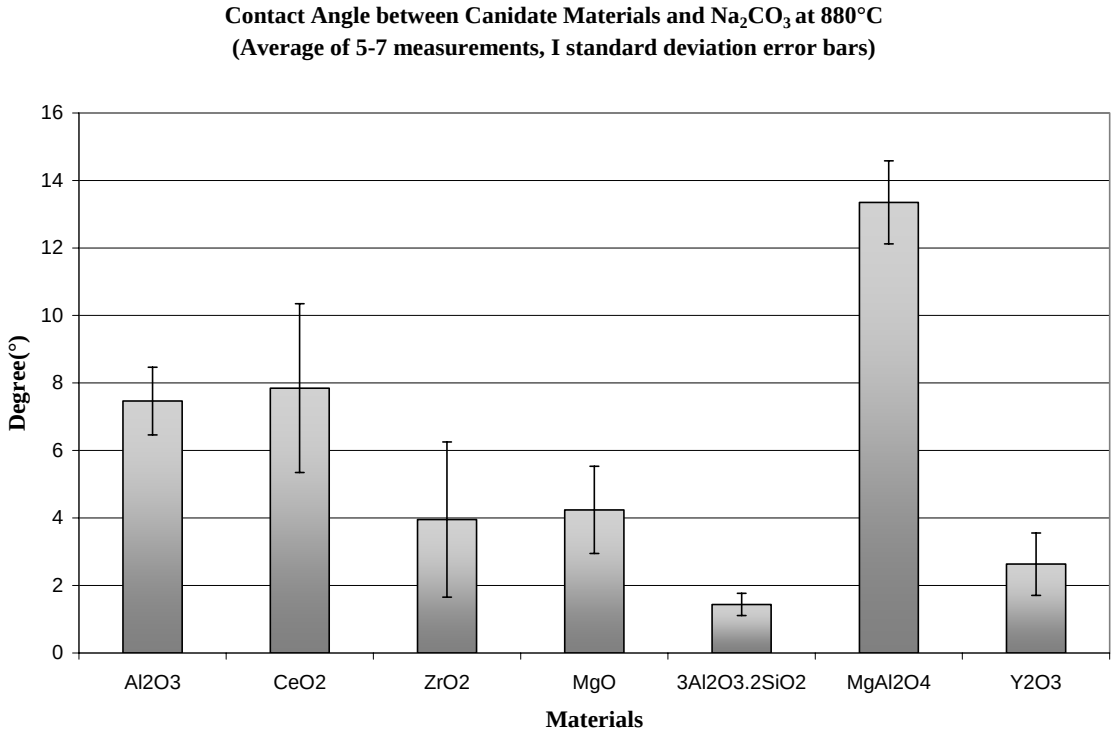

Figure 6: Contact Angle of Na_2CO_3 on dense candidate materials

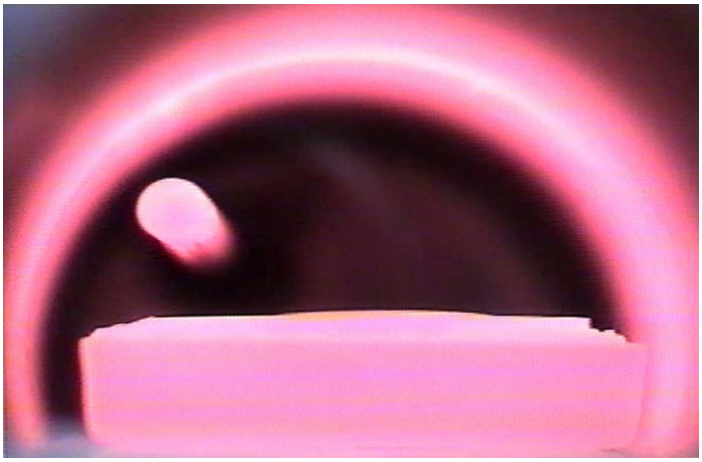

Figure 7: Na_2CO_3 drop on $MgAl_2O_4$ specimen after melting

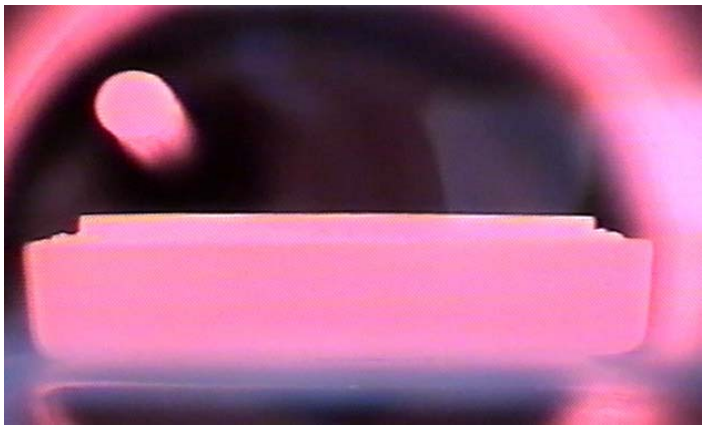

Figure 8: Na_2CO_3 drop on mullite specimen after melting

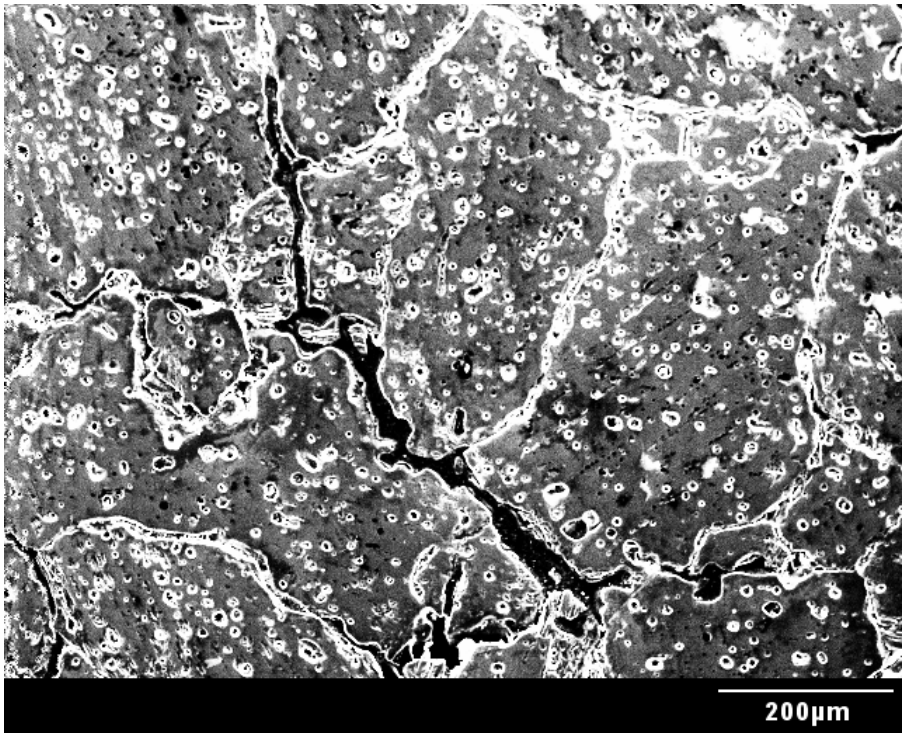

Figure 9: Formation of crack in $LiAlO_2$ substrate due to interaction with sodium carbonate melt (X100/SE/15KV)

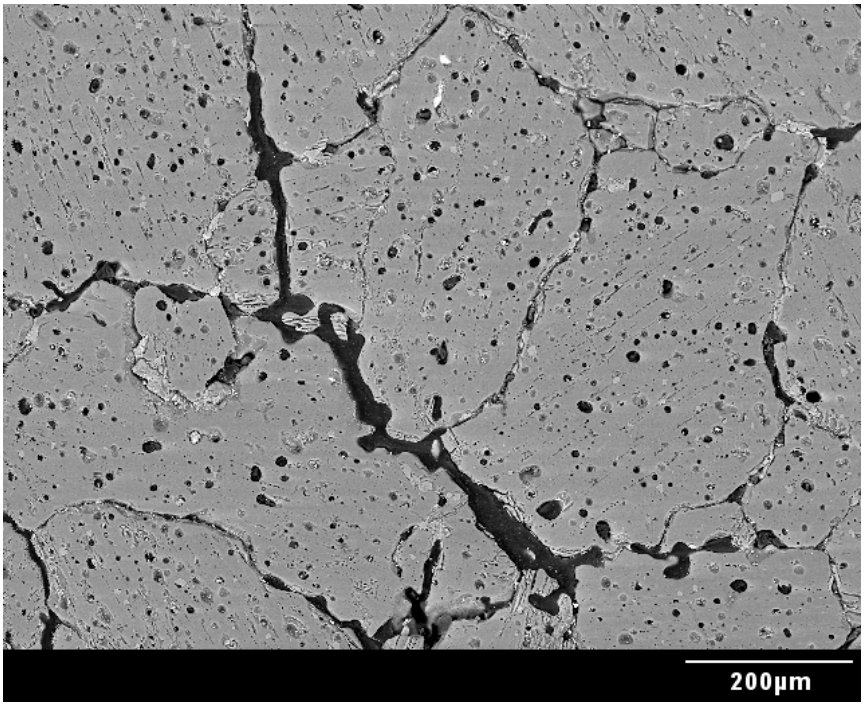

Figure 10: Formation of crack in $LiAlO_2$ substrate due to interaction with sodium carbonate melt (X100/BSE/20KV)

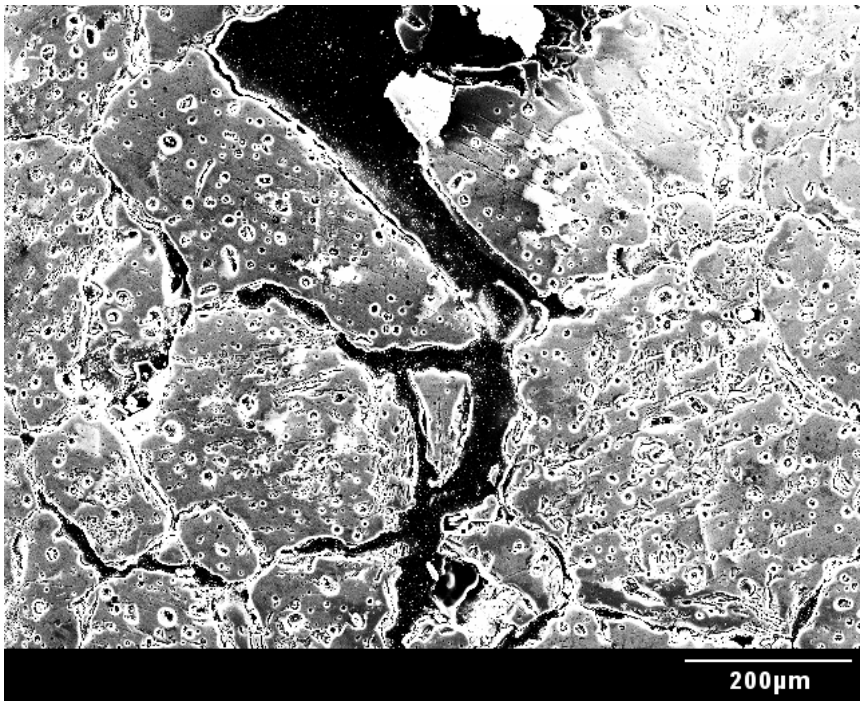

Figure 11: Formation of crack in $LiAlO_2$ substrate due to interaction with sodium carbonate melt (X100/SE/20KV)

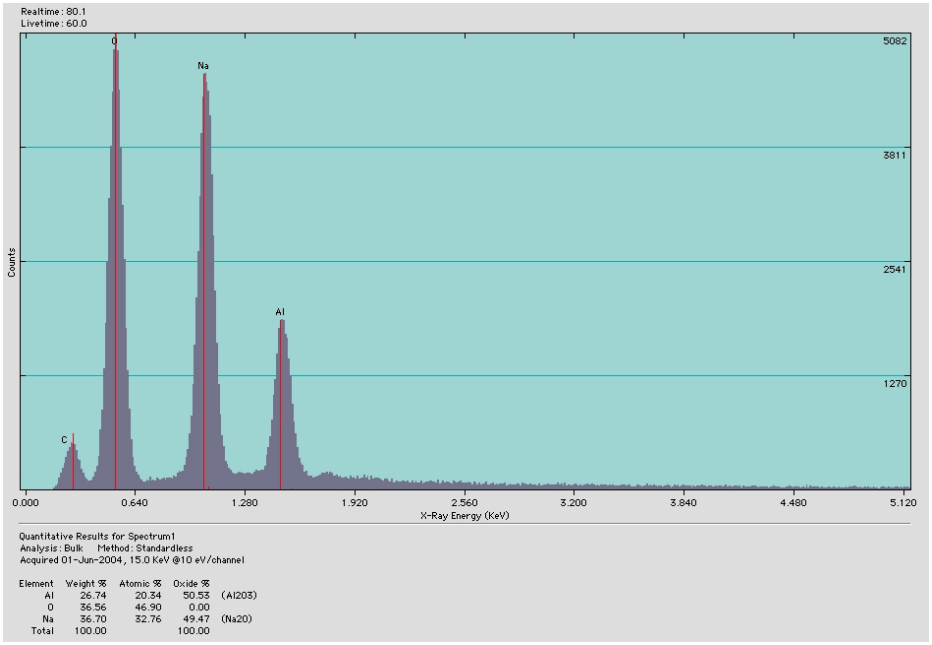

Figure 12: Detection of considerable amount sodium in the areas close to grain boundaries in $LiAlO_2$ substrate

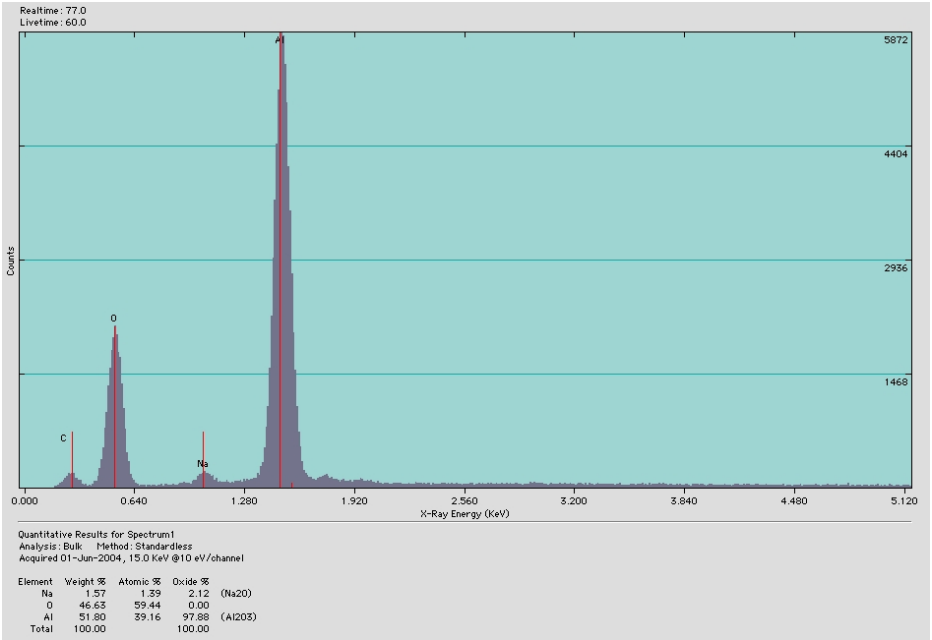

Figure 13: Detection of small amount sodium in grains in $LiAlO_2$ substrate

Formation of cracks in mullite specimen, one of the materials not resistant to sodium carbonate, in the region of the reaction with sodium carbonate was observed as well (Figure 14).

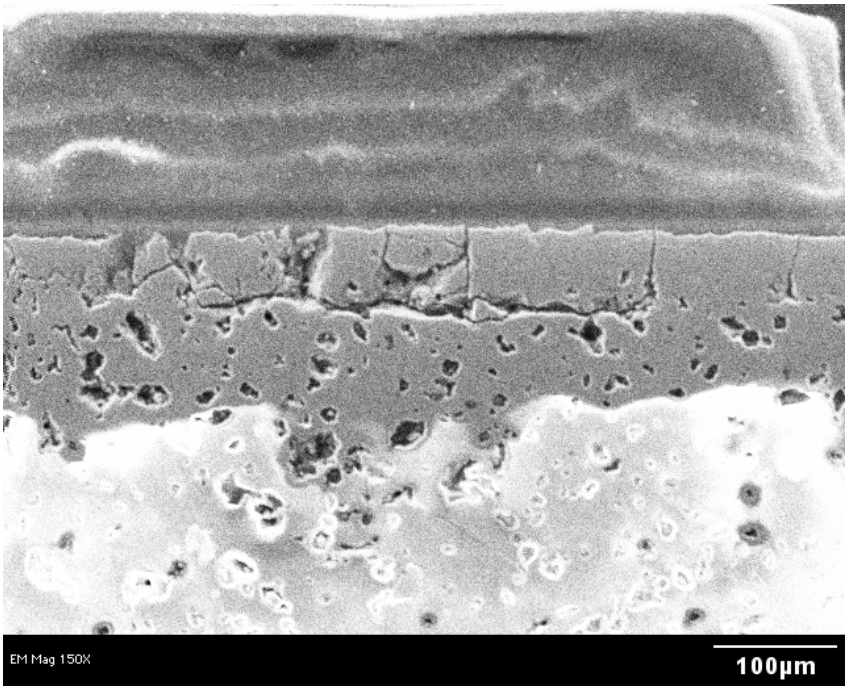

Figure 14: Formation of crack in mullite substrate due to interaction with sodium carbonate melt (X150/BSE/20KV)

Figure 15 is a plot of contact angle between the candidate oxides and potassium carbonate measured to date. In this case magnesium oxide showed the highest wetting angle of about 10 ± 2 degrees.

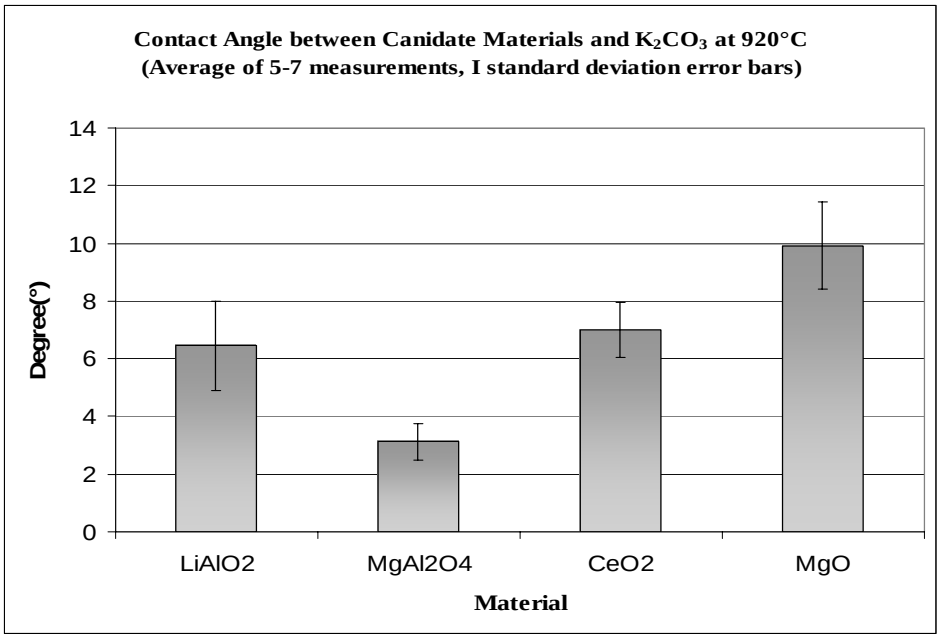

Figure 15: Contact Angle of K_2CO_3 on dense candidate materials

X-ray diffraction was used to determine the reaction products. The depth of beam penetration was varied by controlling the angle of incidence. A low angle of incidence was used to show that the surface coating was indeed sodium carbonate. The surface coating was sodium carbonate for the specimens that did not react. Increasing the angle of incidence increased surface penetration showing sodium carbonate, the original oxide and any reaction products. In some cases it was possible to further increase the angle of incidence to show the original oxide below the reaction zone
Figure 16 shows the formation of reaction product and sodium aluminate between sodium carbonate and alumina as predicted by Fact Sage®. Figure 17 shows the formation of reaction product and sodium aluminum silicate between sodium carbonate and mullite as predicted. Formation of sodium zirconate which was not predicted by Fact Sage® but predicted by Yamaguchi [12] due to reaction between zirconia and sodium carbonate was observed as shown in Figure 18. Figures 19 and 20 show the lack of reaction products with magnesia and ceria as predicted by FactSage®. Figure 21 shows that yttrium oxide in contact with sodium carbonate formed sodium yttrium oxide which Fact Sage® didn't predict. It is observed in Figure 22 that magnesium aluminate spinel precipitated magnesium oxide and formed sodium aluminate in contact with sodium carbonate which is not in agreement with thermodynamic predictions. It seems that the kinetics of reaction is slow between spinel and sodium carbonate at 1000°C because the reaction layer at the surface of the substrate after sessile drop testing was very thin and a relatively thick transparent layer of sodium carbonate smelt had solidified at the surface. X-ray diffraction did not show any reaction between lithium aluminate and sodium carbonate in a powder mixture of the components which agrees with the thermodynamics (Figure 23) but x-ray diffraction from surface of the substrate exposed to sodium carbonate in sessile drop testing shows the formation of sodium aluminate as a new compound (Figure 24). Barium aluminate formed barium carbonate and sodium aluminum oxide in powder

mixtures (Figure 25) at 1000°C under argon. It is predicted that barium aluminate dissociated to barium carbonate and aluminum oxide as the first step and then sodium carbonate reacted with aluminum oxide and formed sodium aluminate.
The materials which didn't show any reaction with sodium carbonate or were among the promising candidates were also tested with potassium carbonate to measure the contact angle and evaluate their reactivity to potassium carbonate. The results showed that both magnesium oxide and cerium oxide were resistant to potassium carbonate as they were resistant to sodium carbonate (Figure 26 and 27) which verified the results of thermodynamic studies. Magnesium aluminate spinel reacted with potassium carbonate and formed magnesium oxide and potassium aluminum oxide as reaction products (Figure 28). Therefore spinel was probably dissociated to magnesium oxide and aluminum oxide first and the reaction between aluminum oxide and potassium carbonate formed potassium aluminate. Also thermodynamics showed that spinel would not be resistant to potassium carbonate. Both lithium aluminate and barium aluminate in powder mixture with potassium carbonate showed no reaction with potassium carbonate as was predicted by Factsage® (Figure 29 and 30) but lithium aluminate substrate exposed to potassium carbonate in sessile drop testing shows some peaks which can be identified as the peaks of potassium aluminate but the formation of new phase cannot be assured (Figure 31).

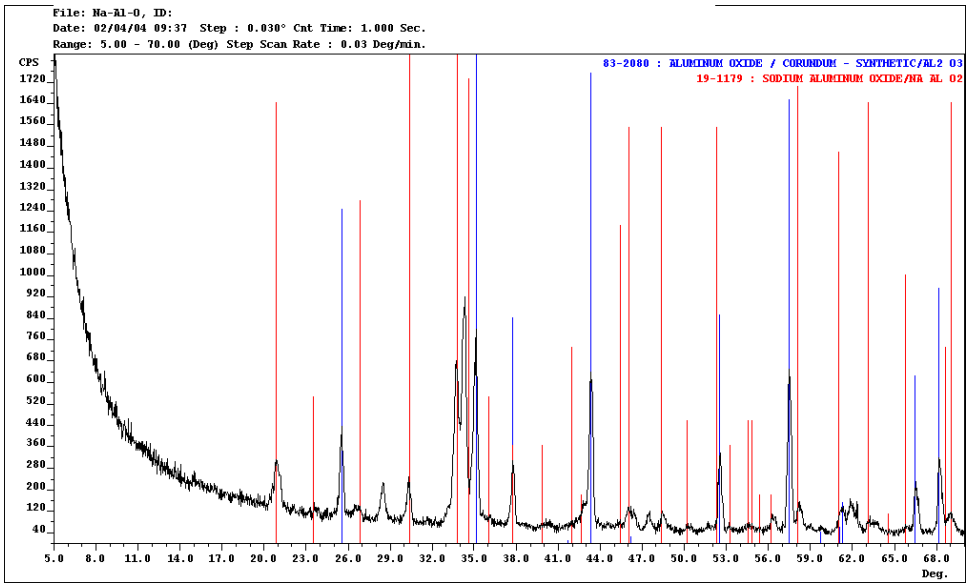

Figure 16: X-ray diffraction pattern showing reaction product sodium aluminate and original corundum

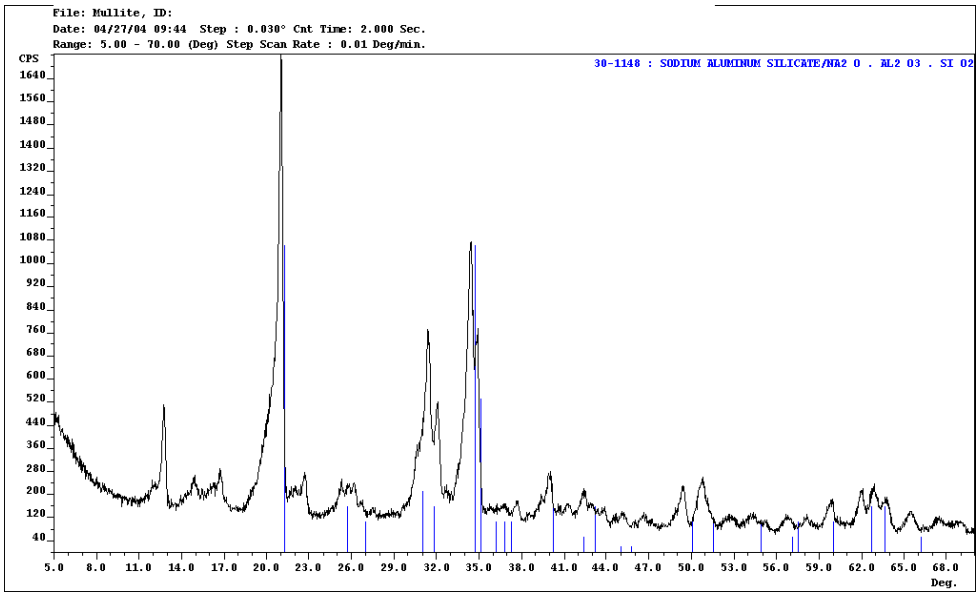

Figure 17: X-ray diffraction pattern showing reaction product sodium aluminum silicate in mullite specimen

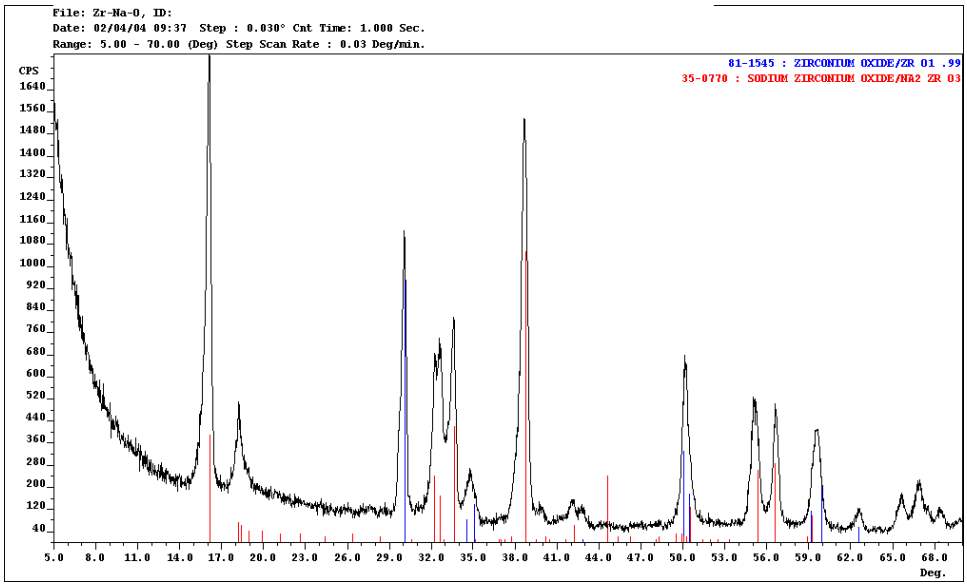

Figure 18: X-ray diffraction pattern showing reaction product sodium zirconium oxide and original zirconia

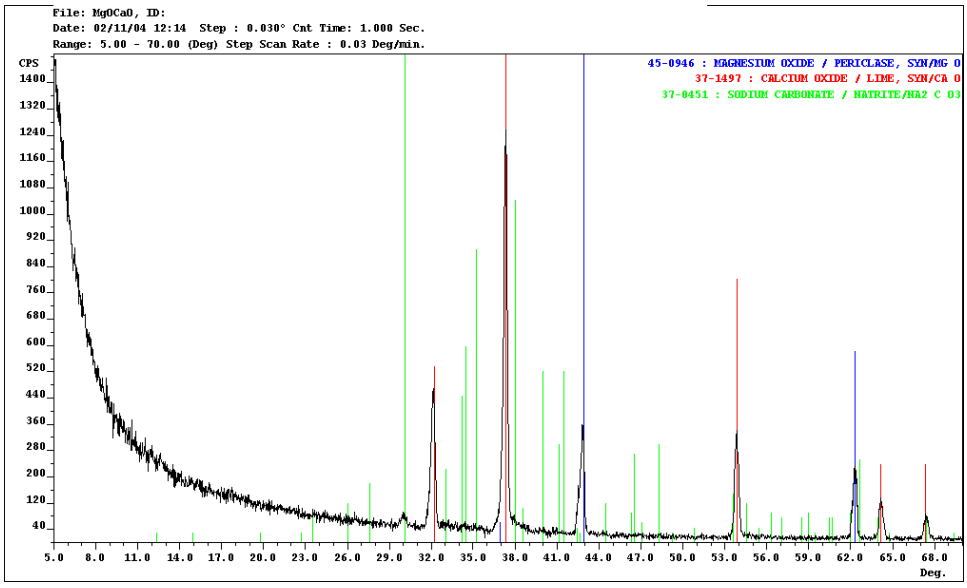

Figure 19: X-ray diffraction pattern showing lack of reaction product with original magnesia, calcia and Na_2CO_3

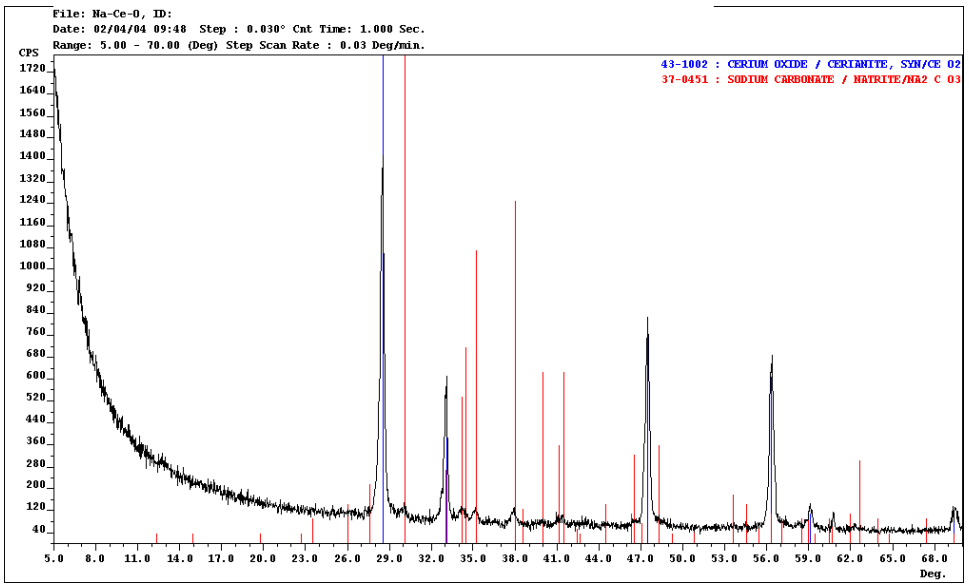

Figure 20: X-ray diffraction pattern showing lack of reaction product with original ceria and Na_2CO_3

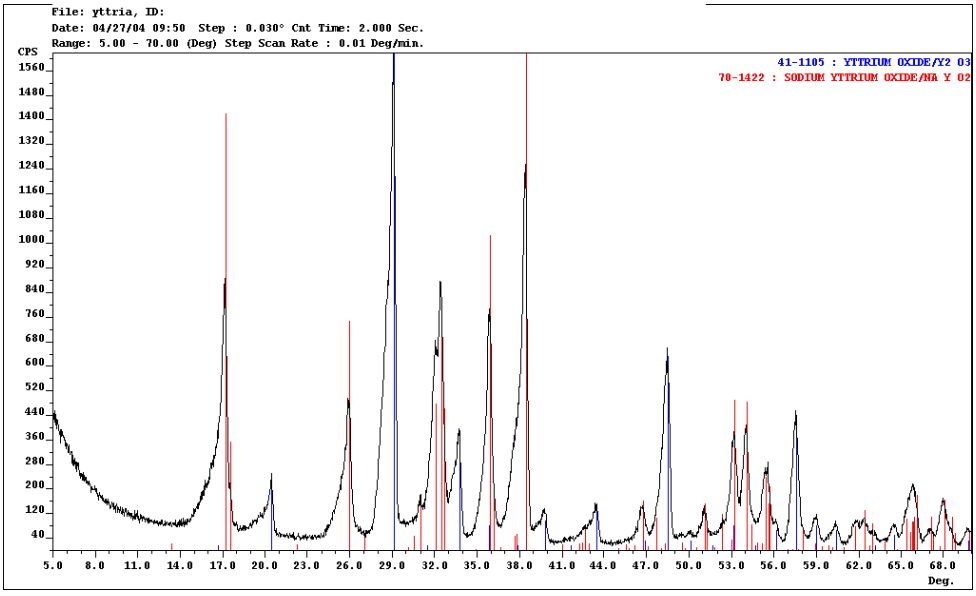

Figure 21: X-ray diffraction pattern showing reaction product sodium yttrium oxide and original yttrium oxide

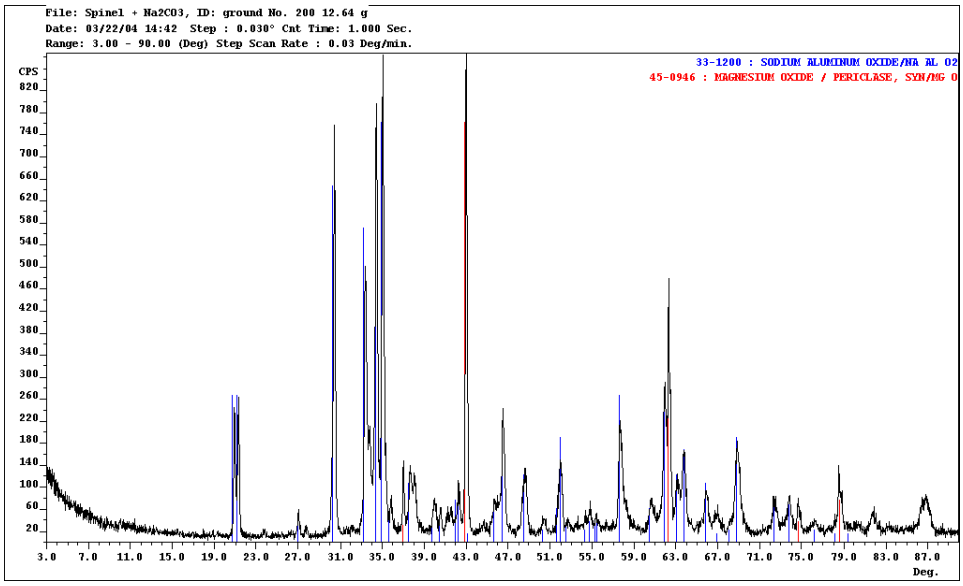

Figure 22: X-ray diffraction pattern showing reaction products sodium aluminum oxide and magnesium oxide in spinel specimen

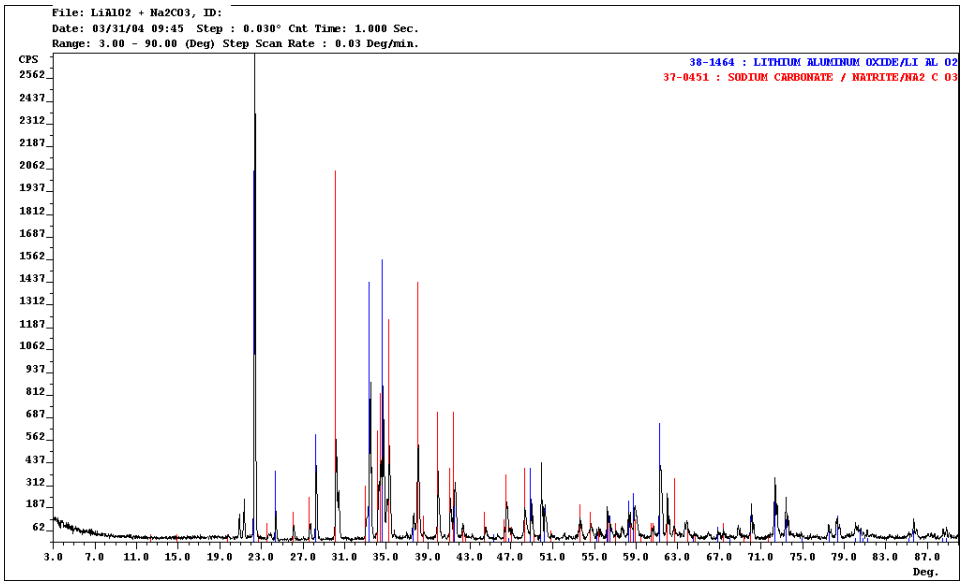

Figure 23: X-ray diffraction pattern showing lack of reaction product with original lithium aluminate and Na_2CO_3 (powder mixture)

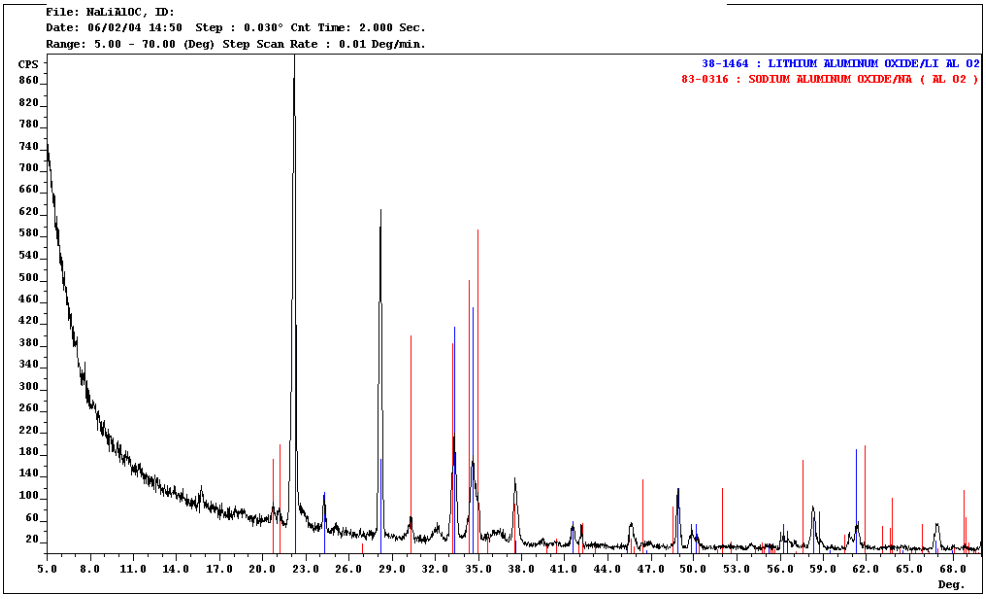

Figure 24: X-ray diffraction pattern showing reaction product of sodium aluminate with original lithium aluminate (Sessile drop testing substrate)

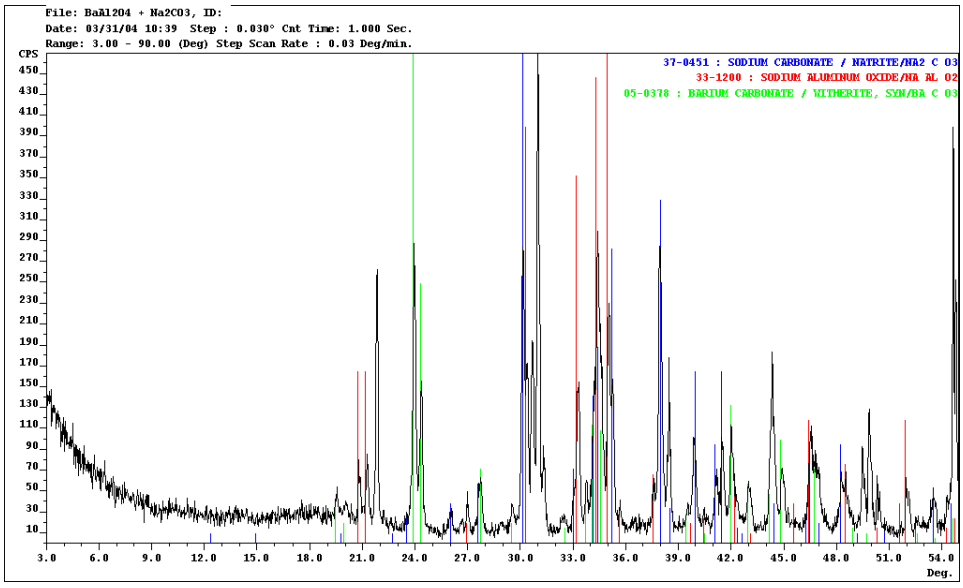

Figure 25: X-ray diffraction pattern showing reaction products of sodium aluminum oxide, barium carbonate and original Na_2CO_3 smelt (powder mixture)

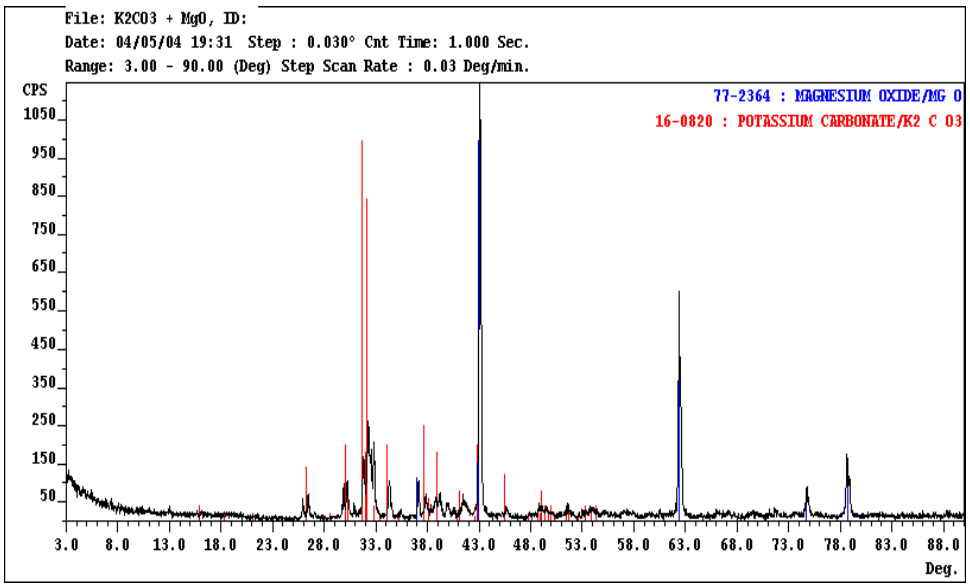

Figure 26: X-ray diffraction pattern showing lack of reaction product with original magnesium oxide and K_2CO_3

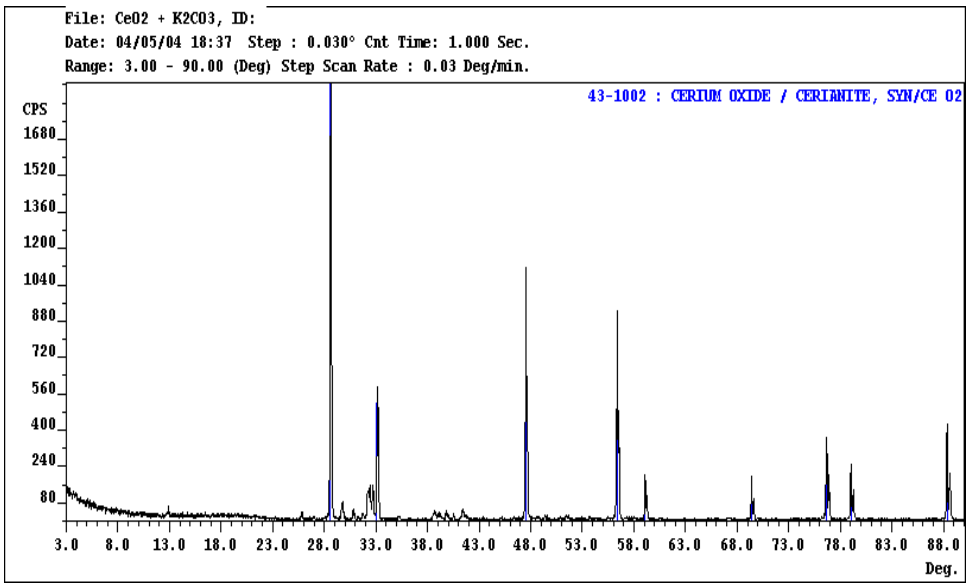

Figure 27: X-ray diffraction pattern showing lack of reaction product with original cerium oxide and K_2CO_3

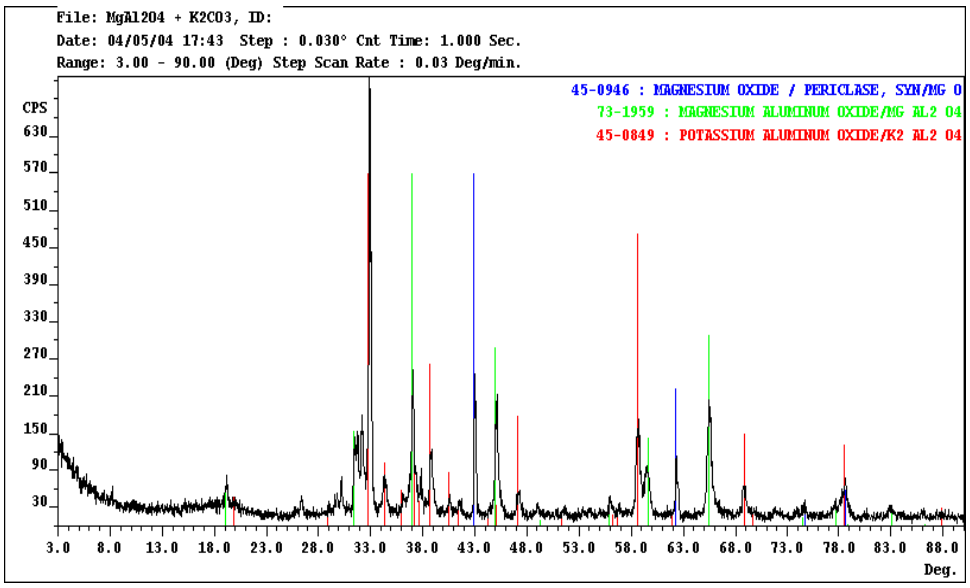

Figure 28: X-ray diffraction pattern showing reaction product potassium aluminum oxide and magnesium oxide, and original spinel

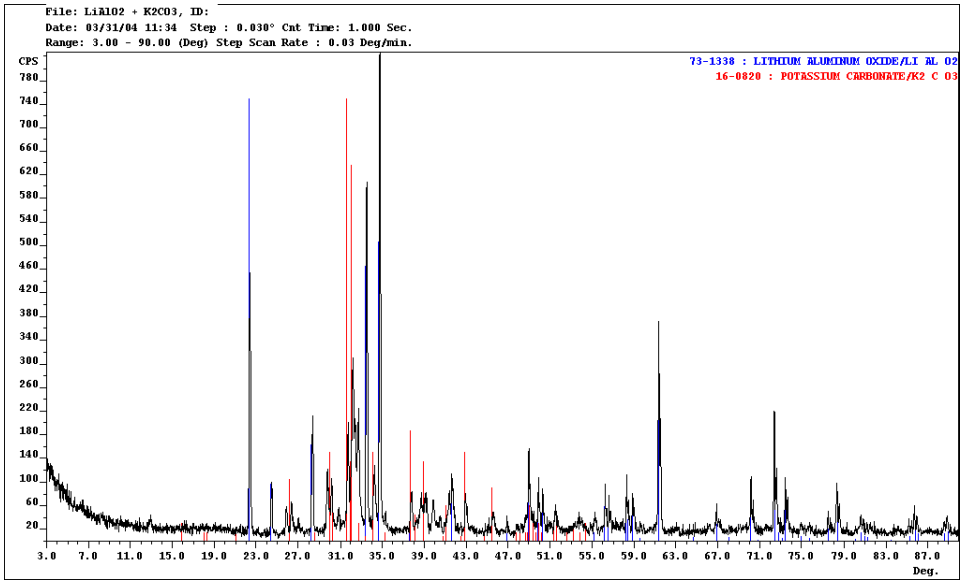

Figure 29: X-ray diffraction pattern showing lack of reaction product with original lithium aluminate and K_2CO_3 (powder mixture)

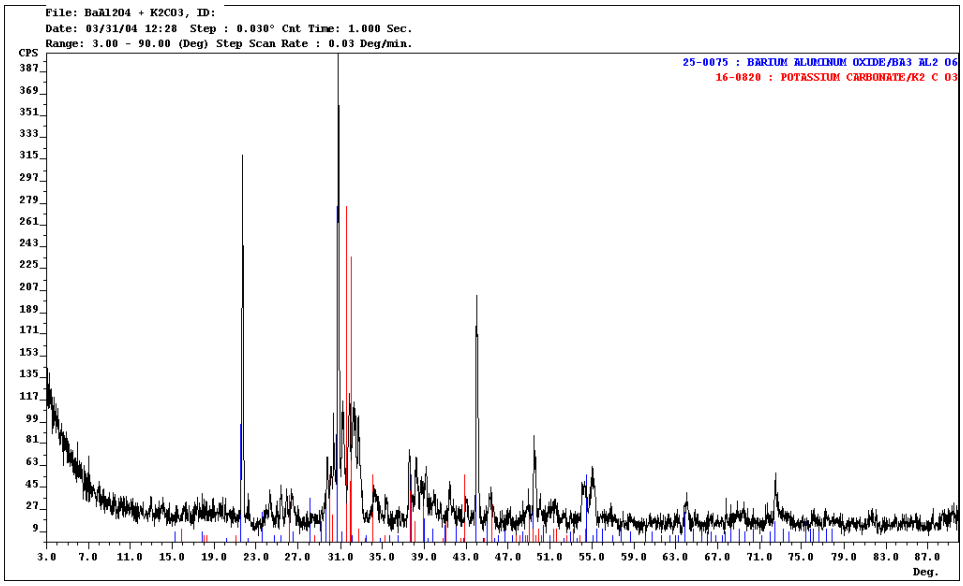

Figure 30: X-ray diffraction pattern showing lack of reaction product with original barium aluminate and K_2CO_3

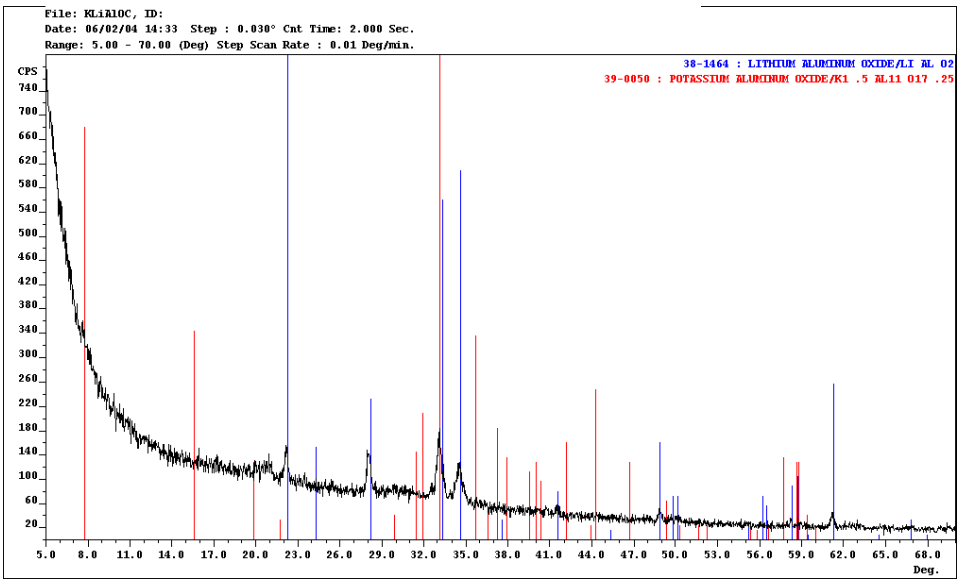

Figure 31: X-ray diffraction pattern showing reaction product of potassium aluminate with original lithium aluminate (sessile drop testing substrate)

The summary of the results from x-ray diffraction analysis of different samples is also presented in Table I and the results from thermodynamics for comparison with results of x-ray diffraction are presented in Table I.

Table I: Results of thermodynamics (FactSage) and XRD analysis at 1000°C

Candidate Material	Na_2CO_3 (Thermodynamics)	K_2CO_3 (Thermodynamics)	Na_2CO_3 (XRD)	K_2CO_3 (XRD)
Al_2O_3	X	X	X	?
$3Al_2O_3.2SiO_2$	X	X	X	?
CeO_2				
ZrO_2			X	?
MgO				
Y_2O_3			X	?
$MgAl_2O_4$		X	X	X
$LiAlO_2$ (powder mixture)				
$LiAlO_2$ (sessile drop test)			X	X
$BaAl_2O_4$ (powder mixture)			X	

(x): Reaction occurred, (?): No experiment,

CONCLUSION

The results of thermodynamics and experiment were in agreement for some candidate materials and were not in agreement for some. Therefore experimental work is always necessary to evaluate the materials for any application and thermodynamic predictions are not generally sufficient. So far magnesium aluminate spinel showed the highest contact angle with sodium carbonate (13 ± 1 degrees) while magnesium oxide showed the highest contact angle with potassium carbonate (10 ± 2 degrees). Although cerium oxide and magnesium oxide didn't show high contact angle with sodium carbonate and potassium carbonate but they didn't show any reaction with either one of the smelts. Therefore if a high purity material with the least amount of impurity is used for making refractory out of MgO and CeO_2 with dense microstructure, they can be promising candidates for application in black liquor gasifiers.

$MgAl_2O_4$ may still be a good candidate for BLG application although powder x-ray diffraction verified the reaction of sodium carbonate and potassium carbonate with spinel. Because sessile drop test showed relatively high contact angle with sodium carbonate and very thin reaction layer although spinel didn't have a high contact angle (3 ± 1) with potassium carbonate.

Lithium aluminate which was considered as a promising candidate before sessile drop testing doesn't seem to be an appropriate material for BLG application. Despite sessile drop testing is not sufficient for making decision about applicability of one material for this application and other experiments need to be accomplished. Contact angle of barium aluminate with both sodium carbonate and potassium carbonate will be measured by sessile drop test and reported along with interaction results.

REFERENCES

1. J. R. Keiser, R. A. Peascoe, and C. R. Hubbard, ”Corrosion Issues in Black Liquor Gasifiers”; pp. 19 in Corrosion/2003 Conference Proceedings, NACE International, San Diego, CA, 2003.
2. L.L. Stigsson and B. Hesseborn, “Gasification of Black Liquor”; Section B, pp. 277-295 in International Chemical Recovery System Proceedings, Montreal Technical Section, CPPA, Toronto, Ontario, Canada, 1995.
3. L. Stigsson, “Chemrec Black Liquor Gasification”; pp. 663-674 in International Chemical Recovery Conference Proceedings, TAPPI Press, Tampa, FL, 1998.
4. C. Brown, P. Smith, N. Holmblad, G. M. Christiansen, and B. Hesseborn, “Update of North America’s First Commercial Black Liquor Gasification Plant”; pp. 33-49 in Engineering and Papermakers Conference Proceedings, TAPPI Press, Nashville, TN, 1997.
5. E. D. Larson and D. R. Raymond, “Commercializing Black Liquor and Biomass Gasifier/Gas Turbine Technology,” *TAPPI J.*, **80** [2], 50-57 (1997).
6. BLG project annual report, 2003.

BIBLIOGRAPHY

W. E. Lee, S. Zhang, “Melt Corrosion of Oxide and Oxide-Carbon Refractories”, A Review from Dept. of Engineering Materials, University of Sheffield, UK., 1999.
V. G. Levich, “Physicochemical Hydrodyanamics”, 1962. Englewood Cliffs, NJ, USA, Prentice-Hall.
W. D. Kingery, H. K. Bowen, D. R. Uhlmann, “Introduction to Ceramics”, Second ed. , John Wiley & Sons. New York, 1976.
R. A. McCauley, “Corrosion of Ceramics”, 1994, New York, Marcel Deker.
M. L. Millard, “The Effect of Microstructure on the Liquid Corrosion of Sodium Chloride and Aluminum Oxide”, Ph.D. Dissertation, Department of Ceramic Engineering, University of Missouri-Rolla, 1982.
Y. Chung, “Corrosion of Partially Stabilized Zirconia by Steelmaking Slags”, M.S. Thesis, Department of Ceramic Engineering, University of Missouri-Rolla, 1993.
C. Wagner, “The Dissolution Rate of Sodium Chloride with Diffusion and Natural Convection as Rate-Determining Factors”, J. Phys. Colloid Chem., 53, 1030-33, 1949.
L. Reed, L. R. Barrett, “The Slagging of Refractories, I. The Controlling Mechanism in Refractory Corrosion”, Trans. Brit. Ceram. Soc, 54, 671-676, 1955.
Y. Kuromitsu, H. Yoshida, “Interaction between Alumina and Binary Glasses”, J. Am. Ceram. Soc, 80 [6] 1583-87, 1997.
L. Reed, L. R. Barrett, “The Slagging of Refractories, II. The Kinetics of Corrosion”, Trans. Brit. Ceram. Soc. 63, 509-534, 1964.
R. Sangiorgi, “Corrosion of Ceramics by Liquid Metals”, NATO ASI Ser., Ser E., Applied Sciences, Vol. 267, pp. 261-84, 1994
N. McCallum, L. R. Barrett, “Some Aspects of the Corrosion of Refractories“, Trans. Brit. Ceram. Soc., 51, 523-543, 1952.
A. R. Cooper, Jr, W. D. Kingery, “Dissolution in Ceramic Systems: I, Molecular Diffusion, Natural Convection and Forced Studies of Sapphire Dissolution in Calcium Aluminum Silicate”, J. Am. Ceram. Soc, 47 [1], 37- 43, 1964.
M. P. Borom, R. H. Arendt, “Dissolution of Oxides of Y, Al, Mg, and La by Molten Fluorides”, Ceramic Bulletin, 60 [11], 1169-1174, 1981.
S. E. Feldman, W. K. Lu, “Kinetics of the Reactions between Silica and Alumino-Silicate Refractories and Molten Iron”, Metallurgical Transactions, 5, 249-253, 1974.
B. N. Samaddar, W. D. Kingery, A. R. Cooper, “Dissolution in Ceramic Systems: II, Dissolution of Alumina, Mullite, Anorthite, and Silica in a Calcium-Aluminum-Silicate Slag”, J. Am. Ceram. Soc, 47 [5] 249-254.
K. McAlister & E. Wolfe, “A Study of the Effects of Alkali Attack on Refractories Used in Incineration”, Proceedings of Incineration Conference, Albuquerque, New Mexico, pp.631-638 (1992).
Yamaguchi, A, “Reactions between Alkaline Vapors and Refractories for Glass Tank Furnaces”, Proceedings of International Congress on Glass, Kyoto, Japan, pp.1-8 (1974).
Thomas, Everett A, “A Study of Soda and Potash Vapor Attack on Super Structure Refractories”, *J. Can. Ceram. Soc*, **44**, 37-41 (1975).
Brown, N.R. “Alkali Vapor Attack of Alumino-Silicate refractories”, Proceedings of International Ceramic Conference: AUSTCERAM 88, Sydney, pp.711-715, (1988).

Kennedy, Christophere R, “Alkali attack on mullite refractory in the grand forks energy technology center slagging gasifier”, *Journal of Materials for Energy Systems*, **3**[N-1, June] 27-31, (1981).
LeBlanc, John R, ”Brockway’s Lower Checker Sulfate Test”, *J. Can. Ceram. Society*, **52**, 58-60, (1983).
Barrie H. Bieler, “Corrosion of AZS, Zircon and Silica Refractories by Vapors of NaOH and of Na_2CO_3”, *J. Am. Ceram. Soc. Bull*, **61**[7], 745-749, (1982).
R. A. Peascoe, J. R. Keiser, “Performance of Selected Materials in Molten Alkali Salts”, 10^{th} International Symposium on Corrosion in the Pulp and Paper Industry (10^{th} ISCPPI); Marina Congress Center, Helsinki, Finland, pp189-200, 2001.
Tadaoki Fukui, “Corrosion of Zircon Refractories by Vapors of Sodium Compounds”, *Ashi Gavasu Kenkya Hokoku*, **17**(2), 77-98 (1967).
J. Gullichsen, H. Paulapuro, “Chemical Pulping, Paper Making Science and Technology”, Book 6B.
J. E. Lazaroff and P. D. Ownby, “Wetting in an Electric Packaging Ceramic System: I, Wetting of Tungsten by Glass in Controlled Oxygen Partial Pressure Atmospheres,” J. Am. Ceram. Soc., **78** [3] 539-44 (1995).
D. A. Weirauch Jr, J. E. Lazaroff and P. D. Ownby, “Wetting in an Electric Packaging Ceramic System: II, Wetting of Alumina by a Silicate Glass Melt under Controlled PO_2 conditions,” J. Am. Ceram. Soc., **78** [11] 2923-28 (1995).
P. D. Ownby, Ke Wen K. Li, D. A. Weirauch Jr, “High Temperature Wetting of Sapphire by Aluminum,” J. Am. Ceram. Soc., **74** [6] 1275-81 (1991).

LIST OF ACRONYMS AND ABBREVIATIONS

BLG=Black Liquor Gasification
LPLT=Low Pressure Low Temperature
HPLT=High Pressure Low Temperature
LPHT=Low Pressure High Temperature
HPHT=High Pressure High Temperature
T_m=melting point temperatura
SEM=Scanning Electrón Microscope
EDS=Energy Dispersive Spectroscopy
XRD=X-Ray Diffraction
T=Temperature